UCRL-52024

MEASUREMENT OF THE NEUTRON SPECTRUM FROM THE REACTION OF 30-MeV DEUTERONS ON A THICK BERYLLIUM TARGET

D. R. Nethaway
R. A. Van Konynenburg
T. M. Adams

February 16, 1976

Prepared for U.S. Energy Research & Development Administration under contract No. W-7405-Eng-48

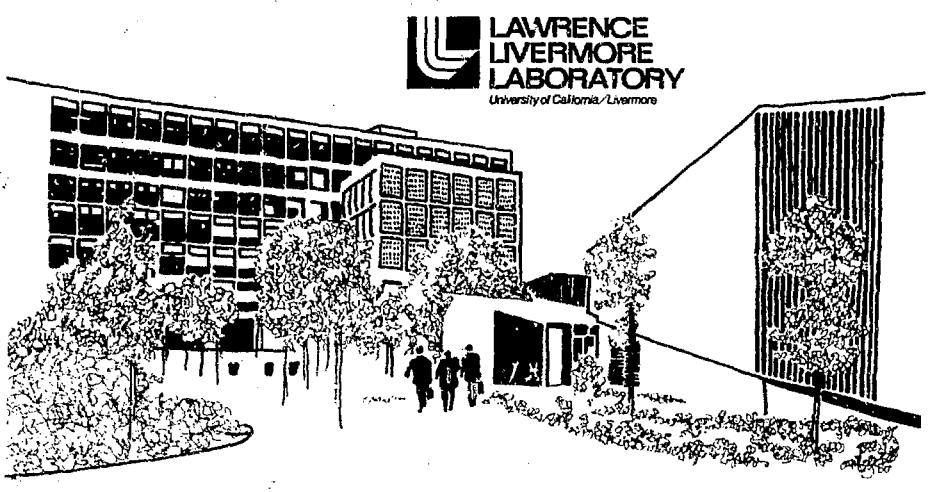

Printed in the United States of America
Available from
National Technical Information Service
U. S. Department of Commerce
5285 Port Royal Road
Springfield, Virginia 22151
Price: Printed Copy $___; Microfiche $2.25*

*Pages	NTIS Selling Price
1-50	$4.00
51-150	$5.45
151-325	$7.60
326-500	$10.60
501-1000	$13.60

Distribution Category
UC-4

LAWRENCE LIVERMORE LABORATORY
University of California Livermore, California 94550

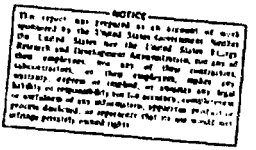

UCRL-52024

MEASUREMENT OF THE NEUTRON SPECTRUM FROM THE REACTION OF 30-MeV DEUTERONS ON A THICK BERYLLIUM TARGET

D. R. Nethaway
R. A. Van Konynenburg
T. M. Adams

February 16, 1976

MEASUREMENT OF THE NEUTRON SPECTRUM FROM THE REACTION OF 30-MeV DEUTERONS ON A THICK BERYLLIUM TARGET

Abstract

We have measured the neutron spectrum produced by bombarding a thick beryllium target with 30-MeV deuterons at the University of California, Davis cyclotron. This spectrum is of interest in studying the effect of neutrons on materials to be used in future fusion reactors. The spectrum was inferred from the activation of two sets of detector foils placed at 0° to the deuteron beam, one immediately behind the beryllium target block, and one 40 mm to the rear. We used a least-squares program to analyze the foil activation data to obtain the fluence in each of seven energy groups. The neutron spectrum (fluence/MeV) close to the target decreases continuously with energy in the range 5-32 MeV, while the spectrum 40 mm back has a peak at about 13 MeV. The contribution from neutrons of energies less than 10 MeV is much greater than that found in previous spectral measurements made at large distances from the target. We attribute this difference to the neutrons which are emitted at large angles from the deuteron beam. These observations show the importance of evaluating the neutron spectrum near the target if samples of materials are to be irradiated in this location.

Introduction

The (d,n) reaction on beryllium provides a source of neutrons that may be appropriate for use in studying the effects of intense fast-neutron irradiation on various materials that are to be used in future fusion reactors. The purpose of this experiment was to examine the spectrum and intensity of the neutrons available at the University of California, Davis cyclotron. A beryllium target was bombarded with 30-MeV deuterons, producing a neutron distribution extending up to about 32 MeV. We have used the foil activation technique in which a set

of foils of various materials is irradiated with neutrons, and the neutron spectrum is inferred from the relative activation of the various foils. We present a preliminary analysis of the measurements in which we have obtained the neutron fluence in each of seven energy groups.

Experimental Details

The irradiation took place at the cyclotron in the Crocker Nuclear Laboratory, University of California at Davis. A beryllium target was bombarded with 30-MeV (±2%) deuterons for 72 min. The beam current varied from 10-23 μA, and the integrated beam current was 0.0865 C.

The beryllium target was a cylinder 3.5 mm thick and 12.7 mm in diameter, held in a copper plate 12 mm thick and 120 mm in diameter. The beryllium was thick enough to completely stop a 30-MeV deuteron. The neutrons born in the target pass on through the rest of the beryllium, an 0.5-mm copper cover, and a 1-mm copper plate containing the cooling water channels.

The deuteron beam was collimated and swept so as to produce a nearly uniform neutron fluence over the detector foils which measured 1.59 × 6.35 mm. The collimator was a tantalum plate with a slot measuring 5 mm in width and 11 mm in total length. The ends of the slot had a 2.5-mm radius of curvature. The beam was swept back and forth a distance of 6 mm with a trapezoidal current in the bending

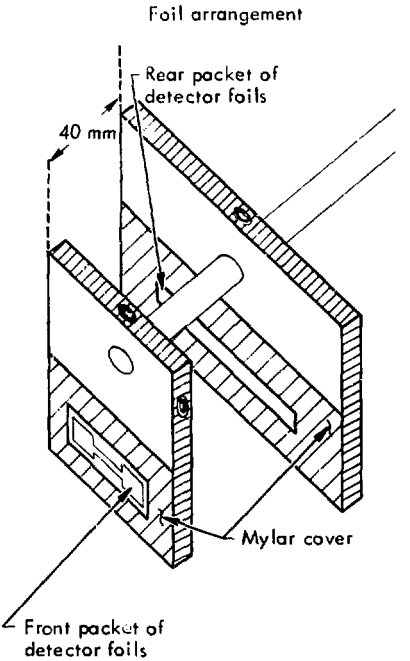

Fig. 1. Diagram showing the arrangement of the front and rear packets of detector foils. The front packet was held against the copper cover plate of the beryllium target assembly.

magnet, such that it paused at each end of the collimator slot for a short time. The ratio of time in transit to time spent at the ends was 4:5.

The arrangement of detector foils is shown in Fig. 1. The front packet of foils was held against the copper cooling plate. The front face of the rear assembly was 40 mm behind. The two target assemblies were placed in epoxy-fiberglass laminate holders attached to a mounting rod and covered with thin sheets of mylar. The front target assembly was centered on the deuteron beam. After the irradiation, the alignment was checked by laying the assembly on photographic film and taking an autoradiograph. The alignment of the small central section of the front foil was found to be off center by about 1.5 mm in the lengthwise direction and almost exact in the other direction.

The foils in the front packet were dumbbell shaped, 9.5 mm wide and 28 mm long, with a central rectangular strip 1.59 × 6.35 mm. This shape is identical to that of the tensile specimens now being routinely irradiated at the Livermore RTNS (ICT) facility. Following the irradiation, the central section was cut away from the larger side strips and used for the radioactivity measurements.

Table 1. Arrangement of detector foils in the two packets.

	Front packet		Rear packet	
	Foil	Thickness (mm)	Foil	Thickness (mm)
1	Al	0.127	Al	0.127
2	Fe	0.127	Fe	0.127
3	Zr	0.127	Zr	0.127
4	Y	0.254	Y	0.254
5	Co	0.254	Tm_2O_3[a]	0.254
6	Al	0.127	Au	0.127
7	Tm_2O_3[a]	0.254	Sc_2O_3[a]	0.254
8	Au	0.127	Al[b]	0.127
9	Sc_2O_3[a]	0.254		
10	Al	0.127		

[a]The Tm_2O_3 and Sc_2O_3 were prepared from thin sheets of the oxide pressed in plastic. Each contained about 70% by weight of the element.

[b]The last Al foil in the rear packet was inadvertently omitted.

The foils in the rear packet were rectangular strips 13 × 48 mm. These foils were used to check the centering of the target holder and to measure the change in neutron spectrum with increasing angle to the deuteron beam. Following the irradiation, these strips were cut into short segments 6.4 mm long for individual radioactivity measurements.

The detector foils in the two packets are described in Table 1. Several aluminum foils were included in the packets so that corrections could be made for the change in neutron fluence going through the foil stacks.

Detector Reactions and Cross Sections

The products from 14 nuclear reactions on the eight target materials were measured. These reactions and their effective threshold energies are listed in Table 2. We attempted to choose reactions whose thresholds and peak cross sections covered all parts of the energy interval up to 32 MeV. However, the number of reactions for which cross-section data exist above 20 MeV is very limited; we used the entire inventory at our disposal. It was necessary to extrapolate the cross sections from 28 to 32 MeV. In most cases, this can be done with sufficient accuracy because of the small neutron fluences at the highest energies. For two reactions, $^{54}Fe(n,\alpha)^{51}Cr$ and $^{59}Co(n,2n)^{58}Co$,

Table 2. Nuclear reactions used for the spectrum determination.

Reaction	Effective threshold (MeV)	Reaction	Effective threshold (MeV)
$^{27}Al(n,\alpha)^{24}Na$	~7	$^{89}Y(n,2n)^{88}Y$	11.6
$^{45}Sc(n,2n)^{44m}Sc$	11.9	$^{90}Zr(n,2n)^{89}Zr$	12.1
$^{54}Fe(n,\alpha)^{51}Cr$	~1	$^{169}Tm(n,3n)^{167}Tm$	15.0
$^{54}Fe(n,p)^{54}Mn$	~1.5	$^{169}Tm(n,2n)^{168}Tm$	8.1
$^{56}Fe(n,p)^{56}Mn$	~4	$^{197}Au(n,4n)^{194}Au$	23.2
$^{59}Co(n,2n)^{58}Co$	10.6	$^{197}Au(n,3n)^{195}Au$	14.8
$^{89}Y(n,3n)^{87}Y$	21.1	$^{197}Au(n,2n)^{196}Au$	8.1

the cross-section data are not complete enough and they were included only as a calibration.

The cross-sections for the 14 reactions used in the data analysis were obtained by evaluating the data available in the literature, and are listed in Table 3. Most of the data are from a recent report by Bayhurst et al.[1] who have made what are probably the most accurate cross-section measurements of this type in the 20- to 30-MeV range, and a comprehensive evaluation of the experimental data up to 20 MeV by Schett et al.[2] The cross sections are given as averages over seven energy groups, and were obtained in a series of iterations by averaging over the spectrum measured for the front foil packet.

Table 3. Group-averaged cross sections used in the data analysis.

		Cross section in millibarns averaged over each group						
Product	References	1-7	7-11	11-14	14-18	18-22	22-26	26-32
^{24}Na	1-4	8.0	66	120	96	42	17.3	5.8
^{44m}Sc	1,5-7			34	149	160	134	93
^{51}Cr[a]	8	6.1	38	72	94	97	77	31
^{54}Mn	2,9	223	470	439	232	104	76	65
^{54}In	2	3.4	57	106	88	48	34	26
^{58}Co[a]	8		19	380	722	730	410	230
^{87}Y	1					0.5	108	58
^{88}Y	1,5-7,10,11			289	1090	1210	1040	574
^{89}Zr	1,5-7,11			186	945	1190	1100	751
^{167}Tm	1,7,11				91	1100	1620	1410
^{168}Tm	1,6,7,11		615	1900	1880	980	441	307
^{194}Au	1						8.0	438
^{195}Au	1				96	1210	1860	1530
^{196}Au	1,5-7		552	1970	2080	1150	474	321

[a]Note that the cross sections to produce ^{51}Cr and ^{58}Co are primarily estimated values, and were included as a calibration.

Results

FOIL ACTIVATION DATA

The radioactivity in the detector foils was measured with a variety of calibrated Ge(Li) detectors.[12] The Sc_2O_3 and Tm_2O_3 plastic foils were ignited, and pure Sc_2O_3 and Tm_2O_3 samples were weighed and prepared for gamma-ray counting. Corrections were made for decay during the irradiation. The final detector results for the front packet are summarized in Table 4. We used the relative activation in the three aluminum foils to correct for the decrease in fluence in the stack of foils; that is, the data for each of the foils were corrected so that the effective fluence would be the same as that in the front aluminum foil. These corrections are included in Table 4.

The foils in the rear packet were cut into short segments 6.4 mm long using an autoradiograph as a guide to find the position of maximum radioactivity. The results for three sets of segments are given in Table 5. The set marked A is the central section of the radioactive area. Sets B and C are the next two 6.4-mm sections to one side. The autoradiograph showed that the maximum activation (the center of segment A) was about 4 mm from the expected center. The rod holding the two foil packets was apparently at a small angle to the deuteron beam.

The data in Table 5 have been corrected for the small (~ 5%) $1/r^2$ decrease in fluence through the foil stack, assuming that the front foil was 43.6 mm from the source of neutrons.

DATA ANALYSIS

The foil activation data were analyzed with SPECTRUM, a computer program that performs a weighted least-squares analysis of the data (atoms/gram and cross sections) to obtain the neutron fluence in energy groups. The SPECTRUM program solves the linear equations $Y_i = K_i \sum_{j=1}^{7} \sigma_{ij} \phi_j$, where Y_i is the measured atoms/gram data, K_i is a conversion factor ($N_A f_i 10^{-24}/AW_i$, where N_A = Avogadro's number, f_i = target isotope fraction, and AW_i = atomic weight), σ_{ij} is the cross section in barns for reaction i in energy group j, and ϕ_j is the fluence (n/cm^2) of neutrons in group j. A number of calculations were made with the SPECTRUM program, trying different energy groupings and varying the number of groups. The group structure used below gave the most reasonable results of those tested.

Table 5. Final detector activation results for the front foil packet. The results are given as atoms of product per gram of detector element.

Product	Atoms/gram	Geometrical correction	Corrected atoms/gram[a]
^{24}Na	1.71×10^{13}	1.00	$(1.71 \pm 0.04) \times 10^{13}$
^{44m}Sc	6.28×10^{12}	1.49	$(9.35 \pm 0.48) \times 10^{12}$
^{51}Cr	3.86×10^{11}	1.03	$(3.96 \pm 1.98) \times 10^{11}$
^{54}Mn	3.72×10^{12}	1.03	$(3.82 \pm 0.23) \times 10^{12}$
^{56}Mn	7.18×10^{12}	1.03	$(7.38 \pm 0.30) \times 10^{12}$
^{58}Co	3.14×10^{13}	1.17	$(3.68 \pm 1.84) \times 10^{13}$
^{87}Y	1.28×10^{12}	1.10	$(1.41 \pm 0.04) \times 10^{12}$
^{88}Y	3.09×10^{13}	1.10	$(3.40 \pm 0.11) \times 10^{13}$
^{89}Zr	1.39×10^{13}	1.05	$(1.47 \pm 0.05) \times 10^{13}$
^{167}Tm	7.23×10^{12}	1.31	$(9.44 \pm 0.42) \times 10^{12}$
^{168}Tm	3.12×10^{13}	1.31	$(4.08 \pm 0.15) \times 10^{13}$
^{194}Au	2.45×10^{11}	1.39	$(3.40 \pm 0.48) \times 10^{11}$
^{195}Au	5.67×10^{12}	1.39	$(7.88 \pm 0.32) \times 10^{12}$
^{196}Au	2.79×10^{13}	1.39	$(3.87 \pm 0.12) \times 10^{13}$

[a]The error assigned to each result is the RMS sum of the statistical uncertainty of the measurement and the overall uncertainty in the cross section. An arbitrary error of ±50% was assigned to the ^{51}Cr and ^{58}Co results because of the large uncertainty in the shape of the excitation function. These errors were used in the least-squares analyses.

The SPECTRUM program results are summarized in Table 6. The neutron fluences in each of the seven energy bins are given for the front foil packet and the three sections from the rear packet. The group 1 and 2 results for segment C have been added together because of a negative result for group 2.

The neutron fluence results were converted to the corresponding neutron spectra by dividing the fluences by the widths of the energy groups. The spectrum for the front foil packet is shown in Fig. 2, in which the fluence/MeV is plotted at an energy corresponding to the middle of the energy group. The spectra

Table 5. Final detector activation results for three sections cut from the rear packet. The results are given as atoms of product per gram of detector element.

Product	Corrected atoms/gram[a]		
	Set A	Set B	Set C
^{24}Na	$(8.09 \pm 0.17) \times 10^{11}$	$(6.66 \pm 0.14) \times 10^{11}$	$(3.44 \pm 0.07) \times 10^{11}$
^{44m}Sc	$(4.48 \pm 0.23) \times 10^{11}$	$(4.00 \pm 0.20) \times 10^{11}$	$(2.30 \pm 0.12) \times 10^{11}$
^{51}Cr	$(1.96 \pm 0.98) \times 10^{10}$	$(1.70 \pm 0.85) \times 10^{10}$	$(9.33 \pm 4.66) \times 10^{9}$
^{54}Mn	$(1.48 \pm 0.09) \times 10^{11}$	$(1.29 \pm 0.08) \times 10^{11}$	$(8.00 \pm 0.49) \times 10^{10}$
^{56}Mn	$(3.66 \pm 0.15) \times 10^{11}$	$(3.16 \pm 0.13) \times 10^{11}$	$(1.70 \pm 0.07) \times 10^{11}$
^{87}Y	$(5.25 \pm 0.17) \times 10^{10}$	$(5.24 \pm 0.17) \times 10^{10}$	$(3.83 \pm 0.12) \times 10^{10}$
^{88}Y	$(1.87 \pm 0.06) \times 10^{12}$	$(1.37 \pm 0.04) \times 10^{12}$	$(7.17 \pm 0.23) \times 10^{11}$
^{89}Zr	$(7.80 \pm 0.25) \times 10^{11}$	$(6.68 \pm 0.21) \times 10^{11}$	$(3.86 \pm 0.12) \times 10^{11}$
^{167}Tm	$(4.40 \pm 0.20) \times 10^{11}$	$(4.09 \pm 0.18) \times 10^{11}$	$(2.62 \pm 0.12) \times 10^{11}$
^{168}Tm	$(2.04 \pm 0.07) \times 10^{12}$	$(1.81 \pm 0.07) \times 10^{12}$	$(9.60 \pm 0.35) \times 10^{11}$
^{194}Au	$(1.05 \pm 0.16) \times 10^{10}$	$(1.28 \pm 0.16) \times 10^{10}$	$(1.17 \pm 0.14) \times 10^{10}$
^{195}Au	$(3.67 \pm 0.15) \times 10^{11}$	$(3.36 \pm 0.14) \times 10^{11}$	$(2.24 \pm 0.09) \times 10^{11}$
^{196}Au	$(1.91 \pm 0.06) \times 10^{12}$	$(1.64 \pm 0.05) \times 10^{12}$	$(9.09 \pm 0.29) \times 10^{11}$

[a]The assignment of errors is described in the footnote to Table 4.

Table 6. Final results for the neutron fluences in every energy groups.

Energy group	Neutron fluence (n/cm^2) in each group			
	Front packet	Segment A	Segment B	Segment C
1-7	$(1.3 \pm 0.2) \times 10^{16}$	$(4.3 \pm 0.9) \times 10^{14}$	$(4.4 \pm 0.7) \times 10^{14}$	
7-11	$(3.2 \pm 0.9) \times 10^{15}$	$(1.3 \pm 0.5) \times 10^{14}$	$(5.4 \pm 3.9) \times 10^{13}$	$(3.5 \pm 0.4) \times 10^{14}$
11-14	$(2.3 \pm 0.6) \times 10^{15}$	$(1.0 \pm 0.3) \times 10^{14}$	$(1.3 \pm 0.3) \times 10^{14}$	$(9.2 \pm 1.3) \times 10^{13}$
14-18	$(2.3 \pm 0.3) \times 10^{15}$	$(1.4 \pm 0.1) \times 10^{14}$	$(8.5 \pm 1.1) \times 10^{13}$	$(2.5 \pm 0.7) \times 10^{13}$
18-22	$(8.7 \pm 3.1) \times 10^{14}$	$(3.6 \pm 1.1) \times 10^{13}$	$(4.7 \pm 1.1) \times 10^{13}$	$(4.5 \pm 0.9) \times 10^{13}$
22-26	$(5.7 \pm 2.2) \times 10^{14}$	$(3.2 \pm 0.8) \times 10^{13}$	$(2.0 \pm 0.8) \times 10^{13}$	$(3.3 \pm 6.6) \times 10^{12}$
26-32	$(2.5 \pm 0.4) \times 10^{14}$	$(7.4 \pm 1.3) \times 10^{12}$	$(9.5 \pm 1.3) \times 10^{12}$	$(9.0 \pm 1.2) \times 10^{12}$

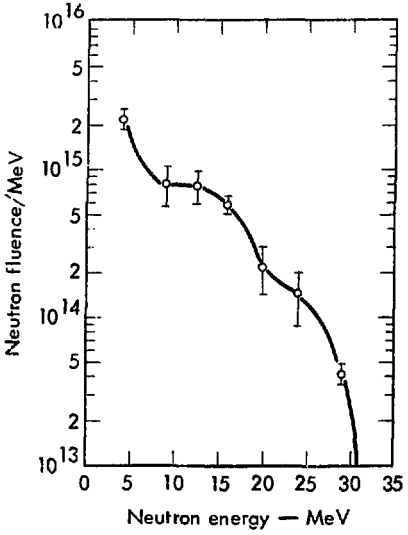

Fig. 2. Neutron spectrum measured for the front detector packet.

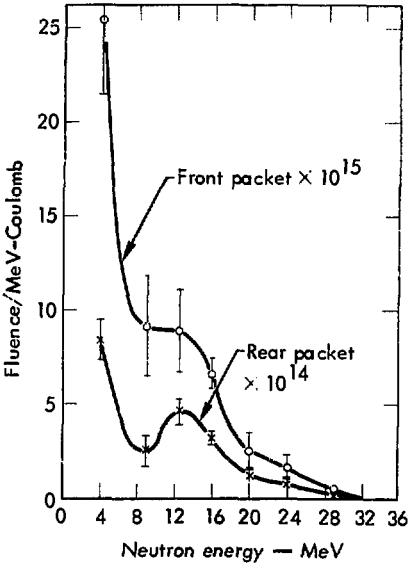

Fig. 3. Average neutron spectrum measured for segments A and B of the rear detector packet.

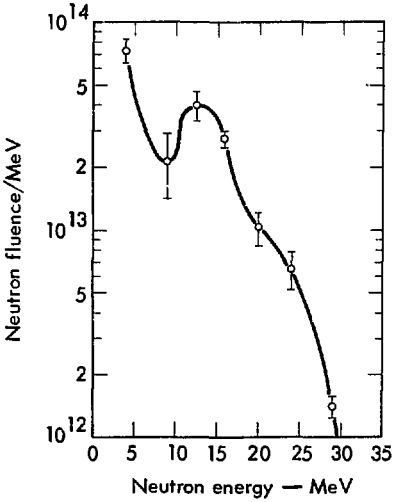

Fig. 4. Linear plot of the neutron spectra (fluence/MeV-Coulomb) versus energy for the front and rear detector packets.

for segments A and B of the rear packet are about the same within experimental error, and the average spectrum is shown in Fig. 3. In this case, the weighted average fluence/MeV for the two segments in each energy group was plotted as in Fig. 2. The data for segment C are somewhat inconsistent with each other, as evidenced by a poor least-squares fit, and the resulting spectrum is unrealistic (and not shown). The two spectra (Figs. 2 and 3) are shown together in a linear plot of fluence/MeV-Coulomb versus energy in Fig. 4.

Conclusions

Since accurate neutron cross-section data in the 20-30 MeV range have not been available until recently,[1] this experiment probably represents the first attempt to measure the shape of a neutron distribution extending to 32 MeV using the foil-activation technique. Several previous measurements have been made of the 0° neutron spectrum resulting from deuteron bombardment of thick beryllium targets with deuteron energies in the neighborhood of 30 MeV.[13-18] Of these, five were performed by the time-of-flight technique in which the detector is placed in "good" geometry, i.e., well-collimated and at a large distance from the target.[13-17] In the sixth, foil activation was used, but the source-sample distance was not given.[18] In general, these previous measurements have yielded a broad peak with a maximum at about 0.4-0.5 of the deuteron energy, and a full width at half-maximum of about 0.35-0.45 of the deuteron energy. In measurements which extended below 4-5 MeV, the neutron intensity was observed to rise slightly at low energies, showing a minimum at this energy. The present results show a much greater contribution from lower-energy (<10 MeV) neutrons, particularly in the spectrum at a point just behind the beryllium target where the peak is not observed at all.

It appears from the present data as well as larger-angle time-of-flight data[19] that this difference can be attributed to the fact that foils placed at a distance from the beryllium target which is less than or comparable to the lateral dimensions of the beam spot are able to intercept neutrons emitted at large angles from the direction of the deuteron beam. These neutrons generally have lower energies than

the forward-directed component because they arise from compound-nucleus interactions, rather than from stripping. As foils are moved back from the target, the lower energy component drops more rapidly than the forward-directed component because of the geometric effect, and the peaked distribution is revealed. These observations show the importance of evaluating the neutron spectrum near the target if samples of materials are to be irradiated in this location.

Acknowledgments

We would like to acknowledge the help and support of Professor John Jungerman and the staff of the Crocker Nuclear Laboratory in performing the irradiation, and the assistance of C. M. Logan of LLL who provided the specially designed beryllium target. We would like to thank Ruth Anderson, Lila Onstott, and Norman Smith for their help with the counter calibrations and data analysis.

References

1. B. P. Bayhurst *et al.*, *Phys. Rev. C* 12, 451 (1975).
2. B. A. Magurno, *ENDF/B-IV Dosimetry File*, Brookhaven National Laboratory, Rept. BNL-NCS-50446 (1975).
3. H. Vonach *et al.*, *Z. Physik* 237, 155 (1970).
4. Y. Kanda and R. Nakasima, *Proc. Conf. on Neutron Cross Sections and Technology*, March 4-7, 1968, Washington, D.C., D. T. Goldman, Ed. (NBS Special Publications 299) Vol. 1, p. 193.
5. R. J. Prestwood and B. P. Bayhurst, *Phys. Rev.* 121, 1438 (1961).
6. D. R. Nethaway, *Nucl. Phys. A* 190, 635 (1972).
7. D. R. Nethaway, unpublished results (1975).
8. M. D. Goldberg *et al.*, Brookhaven National Laboratory, Rept. BNL-325, "Neutron Cross Sections," Vol. IIA, *Z=21 to 40*, 2nd ed., Suppl. No. 2 (1966).
9. R. L. Simons and W. N. McElroy, *Evaluated Reference Cross Section Library*, Battelle Northwest Laboratory, Rept. BNWL-1312 (1970).
10. S. K. Ghorai and W. L. Alford, *Bull. Am. Phys. Soc. II*, 20, 560 (1975).
11. D. G. Gardner, unpublished calculations (1969-1975).
12. R. Gunnink and J. B. Niday, *Computerized Quantitative Analysis by Gamma-Ray Spectrometry. Vol 1: Description of the Gamaral Program*, Lawrence Livermore Laboratory, Rept. UCRL-51061, Vol. 1 (1972).
13. J. P. Meulders *et al.*, *Phys. Med. Biol.* 20, 235 (1975).
14. A. Goland, Brookhaven National Laboratory, personal communication (1976).
15. L. L. Lucas and J. W. Root, *J. Appl. Phys.* 43, 3886 (1972).
16. R. Theus, Naval Research Laboratory, personal communication (1976).
17. S. Johnsen, University of California at Davis, personal communication (1976).
18. I. Heertje and A. H. W. Aten, Jr., *Physica* 30, 978 (1964).
19. K. A. Weaver, *Neutrons from Deuteron Bombardment of Light Nuclei*, Lawrence Livermore Laboratory, Rept. UCRL-51310 (1972), and Addendum (1973).

VRS/11/sg/1a